Visualization of Lead Melting and Solidification Using Neutron Radiography

Partha Sarkar*, Ashish Agrawal, Yogesh Kashyap, Mayank Shukla, Amar Sinha, Lokendra Kumar[1], B. S. Manjunath[1], S. V. Prabhu[2], S.G. Markandeya[3]

Neutron & X-ray Physics Facilities, Bhabha Atomic Research Centre, Trombay, Mumbai, India

[1]Reactor Technology Division, Bhabha Atomic Research Centre, Trombay, Mumbai, India

[2]Indian Institute of Technology, Mumbai, India

[3]Planning & Co-ordination Division, Bhabha Atomic Research Centre, Trombay, Mumbai, India

*rakrasps@yahoo.com

Abstract

Feasibility experimental studies have been carried out on visualization of melting front propagation in real-time for convection driven melting and solidification of lead using neutron radiography facility at CIRUS research reactor. This work has provided with two dimensional radiographs of the propagation of the interface defined by solid and liquid lead with respect to time and heat flux. Specially designed Imaging system comprising of a cooled CCD camera, ^{6}LiF-ZnS converter screen and a front coated Aluminum mirror has been used. Experimental results on pure and impure lead specimen are discussed in this paper.

Keywords

Lead Melting; Neutron Imaging; CCD Camera; Online Visualization; Mushy Region

Introduction

The transport packages of radioactive materials are typically constructed of lead shielding which is filled in steel shells. They are required to meet the performance standards specified by Atomic Energy Regulatory Board (AERB) in India / International Atomic Energy Agency (IAEA) regulations. The principal assurance of safety in the transport of nuclear materials is the design of the packaging, which must allow for foreseeable accidents. Their design has to be such that there should not be any streaming of radiation in case of any accident such as fire. For this reason, the lead casks are subjected to a number of tests to ascertain their performance stability. Subjecting the package to open pool fire test of 800^{0}C for 30 minutes is one such test during which the lead melts followed by solidification. Study of lead melting in transportation packages of radioactive material is very important for estimating their performance during above thermal test. Experimental data related to flow patterns in case of melting and solidification of lead are required for the development of modeling codes with high confidence. Strong non-linearity of the governing equations combined with a moving boundary make a priori prediction of the consequences of inaccuracy or simplifications used in the numerical model almost impossible. As temperature and flow velocity characterizes these types of flow patterns, knowledge about these parameters can be used to deduce information related to solid-liquid phase transitions. Thermocouples have been used by lot of researchers (Emrich, 1981) for measuring the temperature and using it one can ascertain the melting or solidifying front with respect to time. But they are point informative and also destructive in nature as they are placed inside the sample and come in path of the propagating front. A number of studies have been carried out by F Wolf and R. Viskanta in the case of tin and by C Beckermann and R Viskanta in case of gallium. Ultrasound wave based imaging has been proved to be a promising tool for getting temperature information (Sielschott, 1997; Xu et. al, 2002). Ultrasound thermometry based laboratory experiments have been carried by S. Fife et al. for optical and opaque metallic fluids for understanding of the convection flow patterns. Flow velocity measurements using hot wire anemometry, laser Doppler anemometry or ultra sound anemometry has also been reported. Infra-red thermography has been used to obtain the temperature profile at the boundaries of the test specimen and inferences can be drawn about the internal flow process (Carlomagno, 1993). All the above mentioned techniques are somewhat indirect method of interpreting the process phenomena related to its parameters. None had the potential to provide direct images of the solid-liquid interface and its real-time behavior depending upon the external controlling parameters. A lot of computational codes also have been developed and validated with these experiments to predict the interfaces with respect to time and

temperature. The available benchmarking codes are based on experiments carried out using thermocouples and infrared imaging. To obtain two dimensional images with clear demarcation of the solid - liquid phase, one has to adopt attenuation based imaging technique. For light elements such as aluminum and aluminum alloy high energy X-ray radioscopy based experiments have been reported by Yin et al. Patrick G. Barber et al. has also reported X-ray imaging technique for observation of melt-solid interfaces, their shape and movement in germanium and lead tin telluride crystals during their growth. Also gamma ray tomography based studies for the online monitoring of solidification front in metal castings were reported by Jung-Hoon Chun et al. In case of heavy elements like lead, X-ray or gamma ray imaging fails whereas neutrons can easily pass through. Neutrons on the other hand are highly attenuated by material such as hydrogen, water, boron, gadolinium and cadmium. A number of reports are available in flow pattern transition studies of water-air mixture inside metallic pipes, oil flow inside motor engines using NR. Also NR has been used to study water ingress in concrete and metallic composite structures. But lead melting and solidification process and their interface propagation has not been reported till date using direct NR to the best of our knowledge. Flow visualization of solid-liquid interface in Pb-Bi specimens, has been carried by N Takenake et al. and by F. Ogino et al. using NR by tracer induced and dye injection methods. Similar studies related to observation of segregation in Sn-Cd alloy metals using NR have been carried out by H. Reijonen et al. This paper deals with developing real-time neutron radiography technique for visualization and experimental study of lead melting and solidification phenomena.

We have carried out initial feasibility experiments on imaging of solid-liquid interface of lead melting and solidification phenomena using non invasive NR technique. The aim of the study was to visualize the interface during both melting and solidification process and understand the convection driven phenomena. We have visualized the interface transition with respect to time and heating power. These data has provided a great deal of information about the flow patterns depending upon the interface morphology. These flow pattern images can be analyzed for benchmarking of melting process of these types of metallic materials.

Methodology of Nr

This is a non-destructive imaging technique which can produce 2D projection images revealing internal details of bulk materials. Suitable imaging devices are used to record the transmitted intensity of the neutrons through the sample. The intensity recorded by the imaging system can be mathematically written as $\mathbf{I(x,y,t) = G(x,y) * I_0(x,y,t) *exp(-\Sigma \delta)}$, where G is the gain of the imaging system, $\mathbf{I_0}$ is the un-attenuated intensity at x and y (the pixel positions in the image), t is the time, $\mathbf{\Sigma}$ is the total macroscopic cross-section (either of liquid, solid or mixed) and $\mathbf{\delta}$ is the path length traversed by neutron inside the sample. The main assumption in this type of imaging is that "the brightness of the image is proportional to the neutron beam intensity after accounting for dark current and other background corrections". Since lead has a large scattering cross-section which depends upon the material density, the difference of effective $\mathbf{\Sigma}$ is the one that brings out the contrast in these projection images. Solid lead is somewhat transparent to thermal neutrons but not its liquid counterpart as the density of liquid lead is 6% less compared to solid lead. Thus the liquid lead portion produces darker shade than its solid counterpart.

Experimental Setup

The experimentations were carried out at beamline E12 in CIRUS reactor. It is a 40MW research reactor having natural uranium as fuel and heavy water as moderator. The details of collimator, beam line design and shielding aspects are being covered in a separate paper. But for completeness they are briefly discussed here. The beam line is equipped with a specially designed collimator having 16mm opening for neutron beam output from inside of the reactor from a distance of 1.8 meters from its outer shielding wall. Since the L/D of the collimator was 125 it ensured good quality resolution imaging and its special design provided high neutron to gamma ratio. The beam opening was of 120mm diameter. At the sample position the neutron flux was measured to be 3 x 10^6 neutrons /sec. The neutron imaging system was developed using a ^{6}LiF-ZnS converter screen, a front coated aluminum glass mirror and an Andor make cooled CCD camera DW432N. The CCD has 1250x1050 pixels with a pixel pitch of 22 micron and the achieved resolution was ≈ 100 microns. The CCD camera was properly shielded using lead blocks and borated polythene blocks. The schematic of the imaging system is shown in Figure 1(a) and the actual photograph of the installed imaging system in figure 1(b).

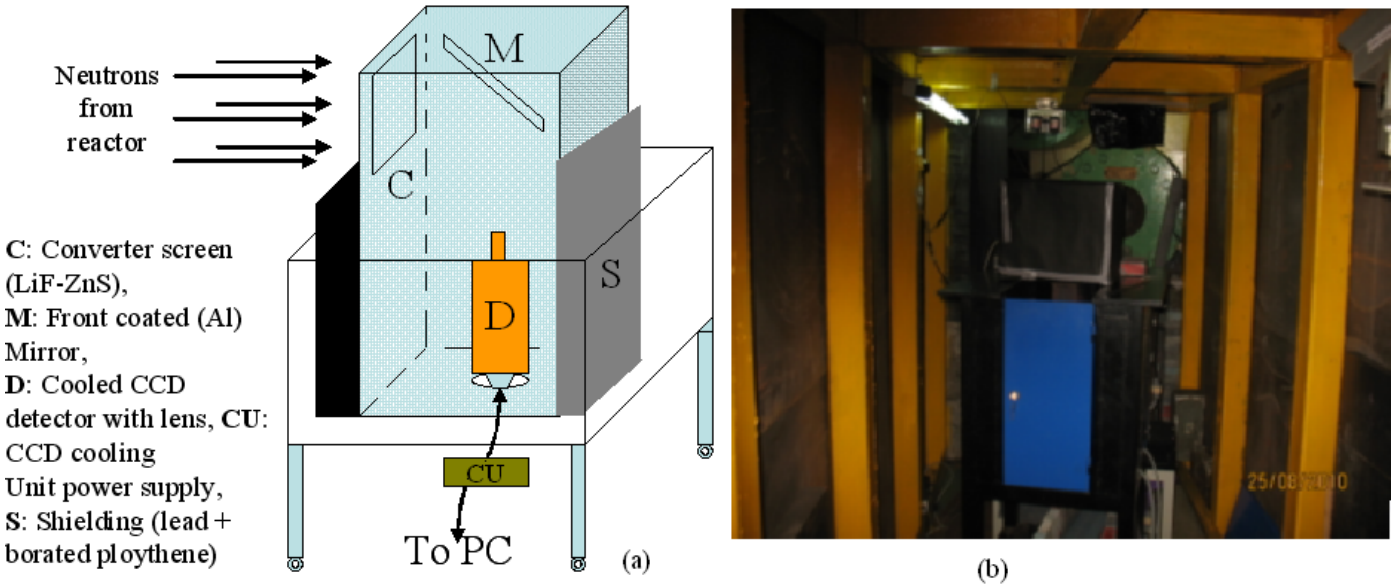

FIGURE 1 (A) SCHEMATICS OF THE IMAGING SYSTEM ALONG WITH ITS COMPONENTS AND (B) THE ACTUAL PHOTOGRAPH OF THE IMAGING SYSTEM AS INSTALLED AT E-12 BEAMLINE, CIRUS. THE IMAGING BOX IS ON TOP OF THE BLUE COLORED TABLE

The CCD camera is connected to a remote PC and its cooling power supply. The data from CCD camera is readout with 1 micro-sec / pixel using frame grabber. Image acquisition software has been developed using Visual C language with various setting options such as acquisition time, detector cooling, different types of data file saving, number of images to acquire etc. The image resolution was computed using its Modulation Transfer Function (MTF) and found out to be 1.64 lp/mm at 10% contrast. The MTF plot is shown in figure 2. A 0.5 mm thick cadmium sheet was placed in contact with the scintillator and its edge response function was calculated, which was then utilized to calculate the MTF of the imaging chain. During the experimentation the CCD chip was thermoelectrically cooled to - 40^{0}C for minimizing the detector noise.

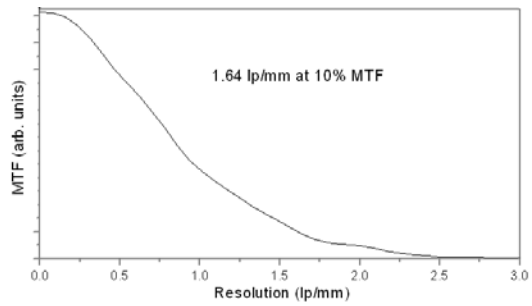

FIGURE 2 PLOT OF MODULATION TRANSFER FUNCTION (MTF) OF THE IMAGING SYSTEM

The lead melting setup was designed keeping in mind the safety issues to be followed in side reactor halls. Figure 3(a) below shows the schematics of the lead specimen of 50 x 50 x 60 mm^3 (B x H x L) size along with the heating element and other parts. The neutron beam is parallel to the 50mm side. The thickness of the test sample was taken because prior experiments using thermocouples and infra red cameras were carried out on it. Figure 3(b) shows the schematics of the heating coil made up of nichrome strip. Figure 4(a) shows the actual photograph of the test specimen assembly and figure 4(b) shows the neutron radiograph of the assembly with all cables and wires coupled with the thermocouples. A small gap is kept on top of the lead block to take care of the volume expansion of molten lead. The heating element is seen on the right side wall of the block. The imaging system is kept 100 mm behind the test specimen along the neutron beam to ensure the safety of the imaging unit as heaters were coupled with the test specimen. The thermocouples shown in the figure 3(a) have been purposefully fixed to monitor the temperatures at the side walls near the imaging system.

The minimum acquisition time has been found out at the beginning of the experiment so that a good quality image with sufficient signal to noise ratio is obtained for this type of real time studies. It was found out to be 10 seconds for image acquisition. Another 1.7 seconds was required for readout and data transfer and an additional time of 2.1 seconds delay for the next acquisition, making successive image acquisition time as 13.8 seconds. Integrated images of 10 seconds were acquired and saved continuously during the heating and cooling period.

Characterization of the Sensitivity of the Imaging System:

Before carrying out our experimentations we did some study related to the sensitivity of the whole imaging

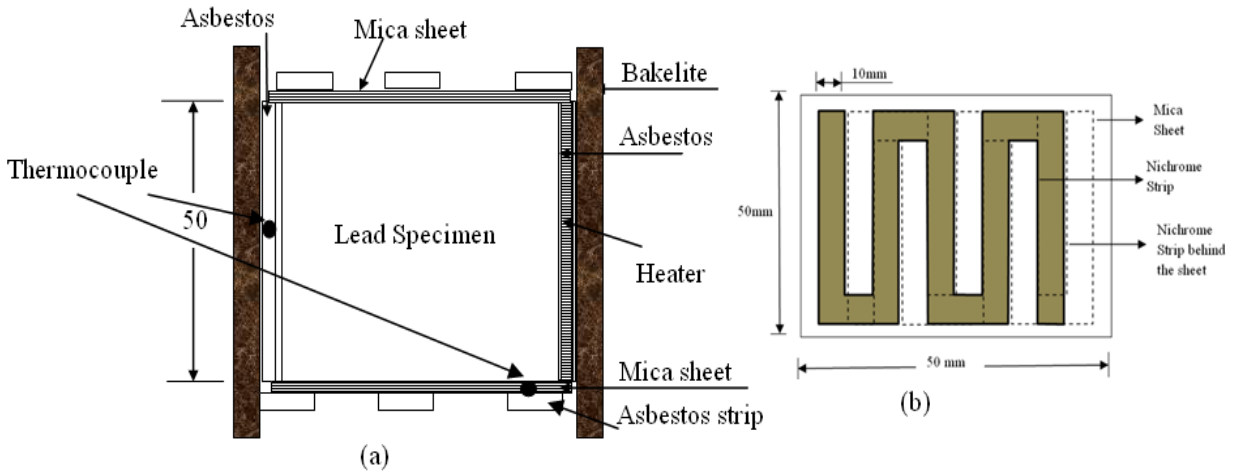

FIGURE 3 (a) SCHEMATICS OF THE LEAD TEST PIECE ALONG WITH ALL THE NECESSARY ELEMENTS SUCH AS BAKELITE, ASBESTOS, MICA SHEET AND THE HEATING ELEMENT. (b) SHOWS THE SCHEMATICS OF THE NICHROME WIRE MADE HEATING COIL

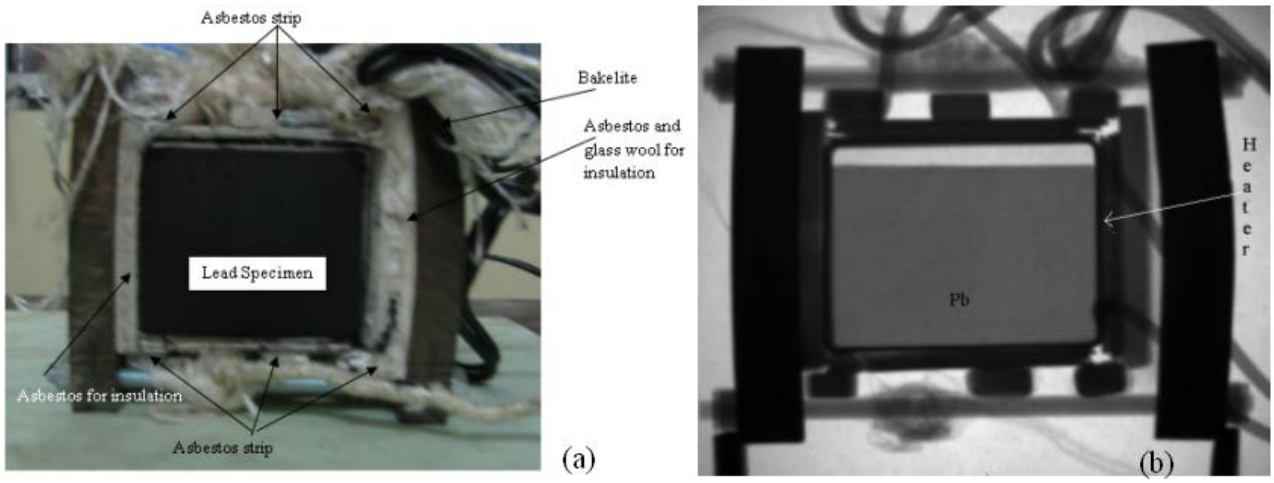

FIGURE 4 (a) PHOTOGRAPH OF THE SAMPLE WITH ALL INSULATIONS AND CONNECTIONS. (b) NEUTRON RADIOGRAPH OF THE TEST ASSEMBLY SHOWING THE LEAD SPECIMEN WITH THE HEATING COIL TO ITS LEFT AND THE CONNECTING CABLES

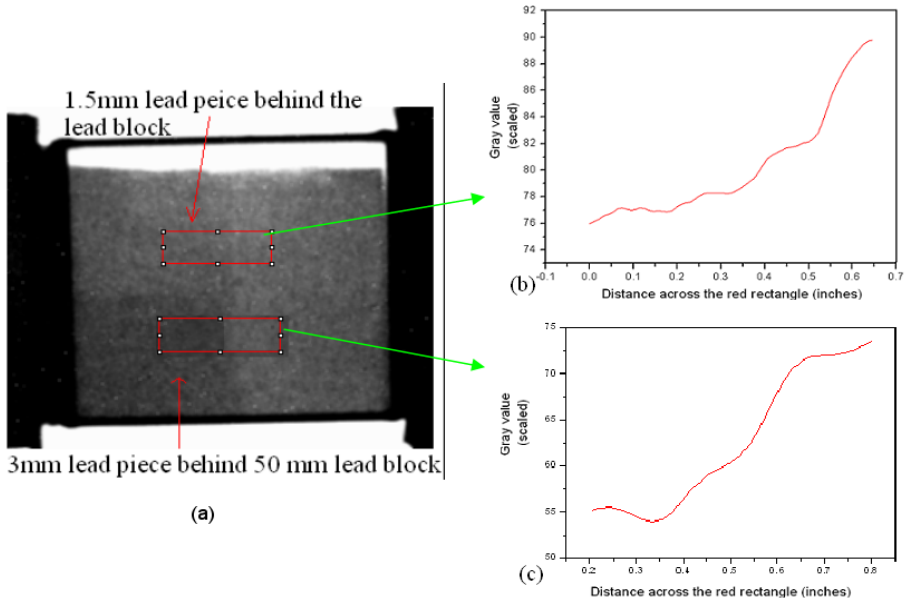

FIGURE 5 (a) NEUTRON RADIOGRAPH OF THE 50MM LEAD BLOCK (TEST SAMPLE) ALONG WITH THE 1.5MM AND 3MM LEAD PIECES PLACED BEHIND IT TO SHOW THE CONTRAST THE IMAGING SYSTEM CAN DETECT, (b) THE AVERAGED LINE PLOT OF MARKED RECTANGLE FOR SHOWING CONTRAST BETWEEN 51.5MM AND 50 MM LEAD AND (c) THE SAME PLOT TO SHOW THE CONTRAST IN CASE OF 53MM AND 50MM LEAD

system. This was carried out by placing two small pieces of lead of thicknesses 1.5 mm and 3mm behind the actual 50mm side of the lead block. The imaging system could distinguish the difference between 50mm and 51.5mm solid lead (providing cumulative density difference of 3%) with 7% contrast and for the 3mm lead piece (providing cumulative density difference of 5.6%) the contrast obtained was approximately 15%. This is shown in figure 5. The shades in the left and right sides of the test piece are evident in the radiography image. Since the density difference between solid lead and liquid lead is around 6% (density of solid lead is 11340 kg/m^3 and that of liquid lead is 10640 kg/m^3), this calibration work gave us the detection sensitivity of this neutron imaging system.

Experimental Results

Experimental Results with Pure Lead Specimen

1) Melting Phenomena

Heating of the test section was carried out at constant rate from one side (in this case – right side wall) with heater power at different constant power levels. The propagation of the melting front and the solidifying front has been seen witnessed with good contrast. Heating of the test section was carried out at constant rate from one side (in this case – right side wall) with heat fluxes at 16.3 kW/m^2 (case 1), 22.7 kW/m^2 (case 2) and 35.1 kW/m^2 (case 3). Figure 6, 7 and 8 shows the melting front propagation in the three cases namely case1, case 2 and case 3 respectively. The solid – liquid interfaces show similar patterns in all the cases but the propagation is faster in case of higher input power. Using the attenuation law the macroscopic attenuation coefficient of liquid lead was found out to be 2.7% higher than its solid counterpart. The image contrast between the liquid and solid portion was found out to be around 15%. The solid/liquid interface was very clearly seen and the morphology of the interface with respect to time has been acquired for analysis. The darker shade is for the liquid part and the lighter shade for the solid part. Using the attenuation law the overall macroscopic cross-section of liquid lead was found out to be 2.7% higher than its solid counterpart. The image contrast between the liquid and solid portion was found out to be around 15%. The molten fraction variation with respect to time has been calculated and shown in figure 9.

The observations for the three cases such as time taken for complete melting, temperature noted by the thermocouple at the opposite side of the heating surface, the onset of the melting process, time taken to start solidification after complete melting and switching off the heaters are tabulated in table 1.

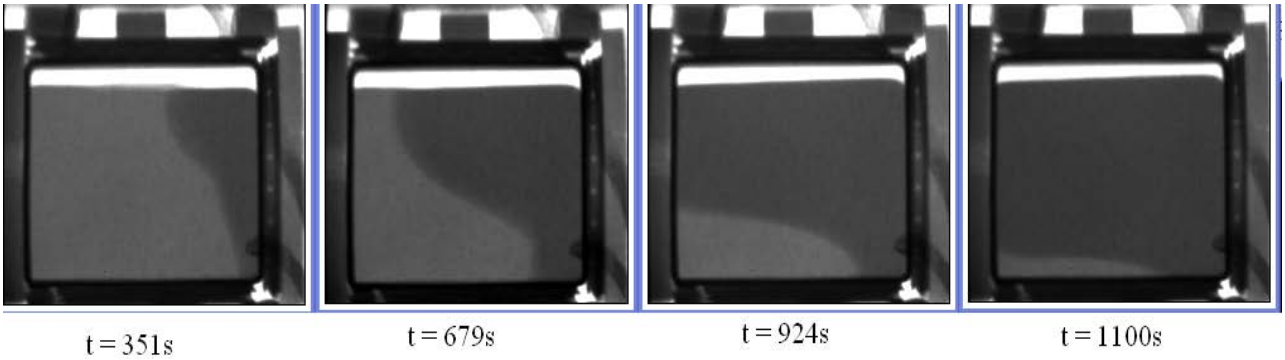

FIGURE 6 NR IMAGES OF MELTING FRONT PROPAGATION AT FOUR INSTANTS FOR CASE 1

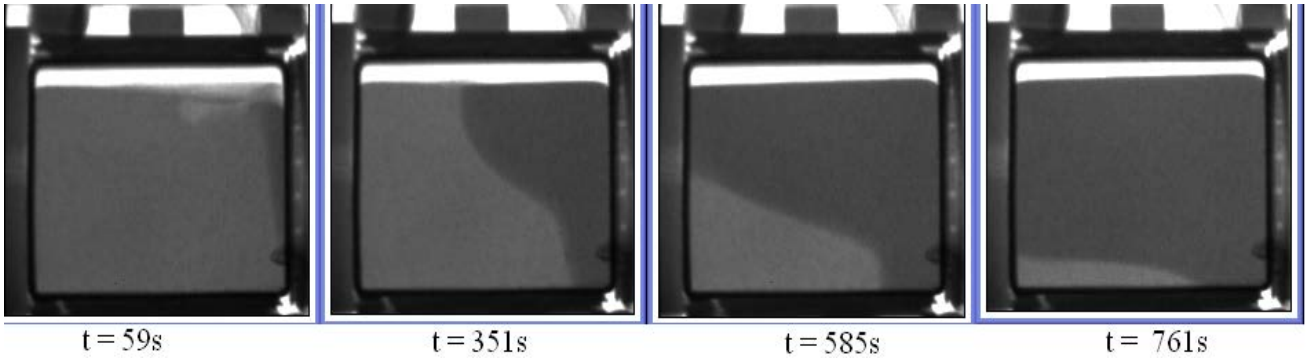

FIGURE 7 NR IMAGES OF MELTING FRONT PROPAGATION AT FOUR INSTANTS FOR CASE 2

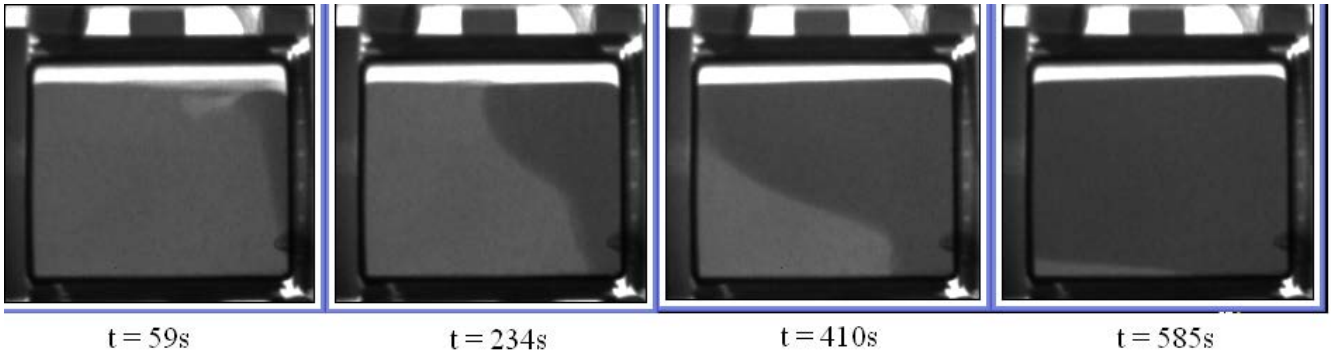

FIGURE 8 NR IMAGES OF MELTING FRONT PROPAGATION AT FOUR INSTANTS FOR CASE 3

parameters	Case 1	Case 2	Case 3
Heating power (kW/m²)	16.3	22.7	35.1
Temperature on the surface opposite to the heating surface at the onset of melting (⁰C)	250±1	246±1	244±1
Total time taken for melting (seconds)	1170	866	526
Total take taken for onset of solidification after total melting and putting the heater OFF (seconds)	117	129	152

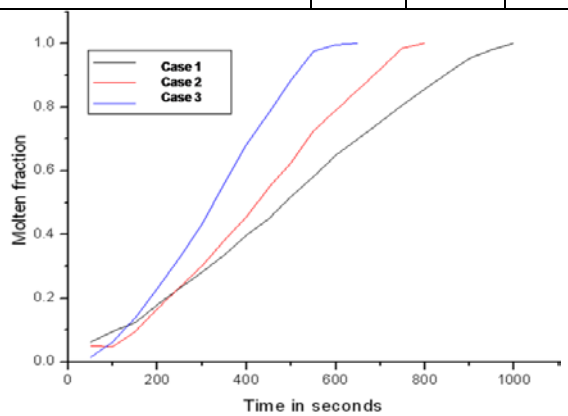

FIGURE 9 PLOT OF MOLTEN FRACTION OF LEAD WITH RESPECT TO TIME AT THREE DIFFERENT HEAT FLUX LEVELS

(16.3 kW/m² (case 1), 22.7 kW/m² (case 2) and 35.1 kW/m² (case 3)).

TABLE 1 TABULATION OF VARIOUS OBSERVATIONS FOR THE THREE CASES

The same sample was also heated from the bottom side by switching the heater from the right side to its bottom face. Transient images of this experiment are shown in figure 10 (a - e) at five different instances. The time zero is taken at the onset of melting phenomena.

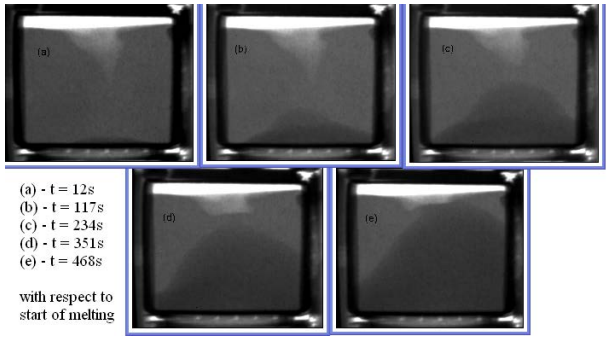

FIGURE 10 (a) – (e) NEUTRON RADIOGRAPHS AT DIFFERENT INSTANCES WHEN THE LEAD SPECIMEN IS HEATED FROM THE BOTTOM SIDE FACE. THE WHITE PORTION (VOID LIKE AT THE TOP), APPEARED AFTER THE FIRST HEATING, REMAINED AT THE SAME LOCATION THROUGHOUT ALL THE EXPERIMENTATIONS.

2) *Solidification Phenomena*

After complete melting of the lead specimen the heater was put OFF and the solidifying process was visualized with respect to time in terms of 2D projection images. Figure 16 shows typical images of the solidifying front at different instances. Figure 11(c-d) shows some void like air pocket on the top portion of the lead specimen during the solidification process. This may be attributed to some re-arrangement of air-pockets in the specimen after its complete melting. This has been seen to appear at the same position irrespective of the heating power. The results in this case are shown in figure 11(a) – (e).

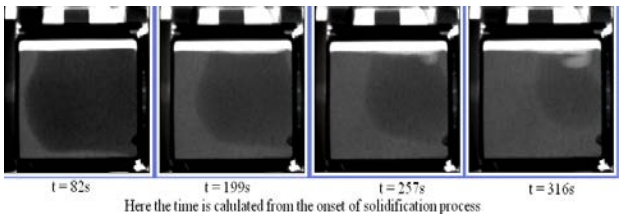

FIGURE11 NEUTRON RADIOGRAPHY IMAGES OF SOLIDIFYING FRONT PROPAGATION AT FOUR INSTANTS OF TIME

Experimentations were also carried out by changing the heating element from right side to the bottom.

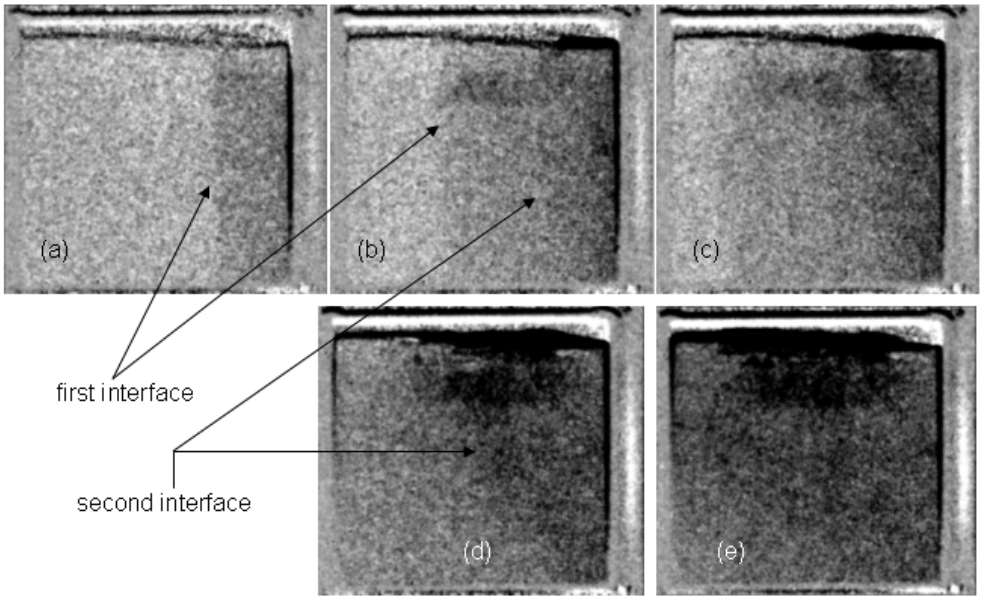

FIGURE 12 (a) – (e) SHOWS NEUTRON RADIOGRAPHS AT DIFFERENT INSTANCES OF TIME IN CASE OF IMPURE LEAD (IMPURITY CAUSED MAINLY BY ANTIMONY)

Experimental Results with Impure Lead Specimen

An experiment was also carried out using impure lead (heated with 150 watts power) and was found out that the interface of the liquid and solid lead is not visible with good contrast. This may be due to the presence of slight amount of antimony in lead, generally used for its rigidity. But with some image processing we could visualize two interfaces at different instances of time. The first interface can be thought as between solid lead and a mixed phase caused due to impurity and the second interface between this mixed phase and the liquid lead portion. The portion between the two interfaces is somewhat the "mushy region" as also described by Hongbin Yen. The image processing involved subtraction of acquired image prior to onset of heating to the images obtained afterwards. Figure 18 shows the interface propagation at different instances of time. Because of the subtraction process for highlighting the feeble features in the transients, the images are noisy. The first interface was seen to be parallel with the side wall from which the heating was carried out and the second interface was seen to follow the same nature as seen in the case of pure lead. The time taken for complete melting was observed to be less compared to the case of pure lead sample.

Conclusion

A highly sensitive real-time thermal neutron imaging system has been developed and applied for feasibility studies on imaging of the interface defined by solid and liquid lead in the case of convection driven lead melting phenomena. The melting front propagation with respect to time and heat flux was imaged using this imaging system. Molten fraction was calculated from the images and was found out to be achieved at a lesser time with higher flux of heat. Visualization of solidification phenomena after complete melting of the lead block at a certain flux level was also carried out. Pure lead samples provided better image quality in terms of contrast rather than the impure one. But in the case of impure sample two interfaces was seen at different instances rather than one in case of the pure lead specimen. In impure sample, the image of a typical "mushy zone" is reported. These feasibility studies can be corroborated with theoretical simulation separately for benchmarking the processes. The detailed analytical approach and comparison with experimental results have been carried out and communicated elsewhere. Future studies related to melting of lead or other important materials with various degrees of impurity can be carried out.

REFERENCES

Barber, Patrick G., Crouch, Roger K., Fripp Jr., Archibald L., Debnam Jr., William J., Robert F. Berry Jr., Richard, Journal of Crystal Growth, 1986;74, 228-230.

Beckermann, C. and Viskanta, R., Journal of Heat Transfer, Vol 111, pp 416 – 424, May 1989; F. Wolff, C. Beckermann

and R. Viskanta, Expermental Thermal and Fluid Science 1988; 1, 83-91.

Chalovicha, T.R., Bennett, L.G.I., Lewis, W.J., Brenizer Jr, J.S., Applied Radiation and Isotopes 61 Pp 693–700, 2004.

Chun, Jung-Hoon, Lanza, Richard C., Saka, Nannaji and Hytros, Mark M., Annals of the CIRP, Vol. 44/1/1995.

Fife, S., Andereck, C.D., Rahal, S., Experiments in Fluids 2003; 35, 152–158.

IEEE Transactions on Nuclear Science, 2005; Vol 52 No.1.

Kanematsu, M., Maruyama, I., Noguchi, T., Iikura, H. and Tsuchiya, N., 3rd ACF International Conference-ACF/VCA 2008, C.16, Pp 925-931.

K., Mishima, S., Fujine, K., Yoneda, K., Yonebayashi, K., Kanda and H., Nishihara, Proc. Japan-U.S. Seminar on Two Phase Flow Dynamics, Ohtsu, Japan, 1988; pp C.3-1.

K., Mishima, T., Hibiki, H., Nishihara, Int. J. Multiphase Flow, No.1, 115, 1993.

Ogino, F. and Kamata, M., Neutron Radiography, Kluwer, Dordrecht, Ed: J.P.Barton, 4th edn 1994, pp 339-346.

Proc. Seventh World Conf. on Neutron Radiography, 2002; Rome, Italy, Sept 15-20.

Reijonen, H. and Forsten, J., Journal of crystal growth 1972; 12 Pp 61-62.

Takenake, N., Jujii, T., Ono, A., Motomura, Y. and Turuno, A., Fusion Engineering and Design 1995; 27, pp 607 – 613.

Wolf, F. and Viskanta, R., Experimental heat transfer, 1987; vol 1, pp. 17-30; Xiaodong Wang and Yves Fauelle, Int. Journ .of Heat & Mass Transfer 2009; 52, 5624-5633.

Yen, Hongbin and Koster, Jean N., Journal Crystal Growth, 2000; 217, pp 170-182.

Yin, Hongbin and Koster, Jean N., Journal of Alloys and Compounds, 2003; 352, pp 175-189.